ATR-FTIR SPECTROSCOPY: ITS ADVANTAGES AND LIMITATIONS

Jože Grdadolnik
National Institute of Chemistry, Hajdrihova 19, SI-1000 Ljubljana, Slovenia

Abstract

In this article the main advantages and limitations of the ATR[*] technique are presented. As examples, the ATR spectra of liquid bulk water and a water solution of protein bovine serum albumin are used. The main differences between the normal transmission spectroscopy and ATR are pointed out. Also shown is the way to calculate the optical constant, using the CIRCLE[™] ATR liquid cell, and from optical constants how to calculate ε' and ε'' as well as pure absorbance spectrum, which is fully comparable with the normal transmission ones

Introduction

Transmission FTIR is the IR method most commonly used in biophysical studies. However, there are a number of technical difficulties commonly encountered with this technique that can make collection of high quality spectra difficult. These difficulties are usually expressed using liquid samples. In normal transmission technique (angle of incidence is equal zero) it is very difficult to ensure the reproducibility of the spacer thickness. This is of the main importance when a solvent such as water is used. Water is known as an extremely good absorber with a molar absorptivity of 104.4 M^{-1} cm^{-1} in the 3µm range. This characteristic of water and in general of H_2O molecules often leads to signal saturation. The smallest commercially available cell spacers, which are 6 µm thick, produce an absorbance near 3 absorbance units, where a linearity of all commercial known detectors is corrupted. In other words that means that the region between the 2800 cm^{-1} and 3700 cm^{-1} is completely without useful information. Furthermore, bands, which have their position in the mentioned region, are fully overlapped with usually much broader and intense OH stretching and hence are lost for further exploitation. Because of a non-linear detector response the subtraction is useless. Therefore, the spacer thickness should be reduced to avoid saturation effects. This is

---

[*] **Abbreviations**: ATR attenuated total reflection, IRE internal reflection element, FTIR Fourier transform infrared, IR infrared, K-K Kramers-Krönig transformation, BSA bovine serum albumin
[™] **CIRCLE** is trademark of Spectra-Tech, Barnes Analytical Division

typically below 1 μm for dilute water solutions. However, using such thin spacers causes problems with reproducibility. Generally, it is not trivial to fill such liquid cells without air bubbles incorporated in the sample. Concomitant with reducing the spacer thickness, we also approach to the limit where the effects of the surface water are not negligible, i.e. the interaction of surface water molecules (or other solvent used) with the window material may become important, and may significantly alter the spectrum of "bulk sample".

An alternative solution of described problems represents attenuated total reflection (ATR)[1,2]. In this method a solid or liquid sample must be brought near the optical element where a light is totally internally reflected and where the sample interacts with the evanescent wave. The effective path length for this interaction depends on several parameters and is typically a fraction of a wavelength. Because of the small light penetration depth, the ATR technique is ideal for highly absorbing samples and for surfaces and thin film measurements. Generally, the ATR spectra are similar to regular transmission; however, for thick samples when spectra are recorded at angles greater than the critical one, the wavelength dependence is observed. Penetration depth d_p is hence equal to

$$d_p = \frac{\lambda}{2\pi n_r \sqrt{\sin^2(\theta) - \frac{n^2}{n_r^2}}} \qquad (1)$$

where λ is vacuum wavelength of the radiation, n_r and n are the real refractive indices of the IRE and sample, respectively, and θ is the angle of incidence. Moreover, ATR spectra possess not only the absorption features, but also the reflection ones. Therefore ATR spectra can not be used in quantitative manner (band shape analysis, determination of oscillator strengths,…) directly. To obtain the absorption spectrum, we have to separate both contributions, i.e. optical constants n and k should be calculated. After this operation, spectra recorded in normal transmission mode can be fully comparable by those recorded in ATR setup. The optical constants of materials can be precisely determined by combining measurements made at different angles of incidence. Most commercial ATR cells do not have the possibility to change the incident angle. Hence to calculate the optical constants, an alternative procedure called Kramers-Kronig (K-K)

methods should be used[3-5]. This method is based on the interdependence of the optical constants by integral relation and on the use of Fresnel's equations.

In this paper the main differences between absorption and ATR spectra will be discussed. These differences will be presented on two examples, i.e. liquid water and dilute protein (bovine serum albumin, BSA) in phosphate buffer. We used these two systems first to demonstrate the differences between the rough ATR spectra and calculated spectra and second to present how to calculate the absorption spectrum from reflection one. Since, the widely acknowledged $1/\tilde{v}$ effect on ATR absorbance, which is usually served as *ATR correction* in commercial software, is not the only distortion in ATR spectrum, the influence of so called *anomalous dispersion* must be taken into account.

Background

Since the optical constants are known, it is very easy to calculate both real (*n*) and imaginary (*k*) dielectric constant and absorption spectrum (*A*). From a known *k*, the absorption spectrum can be expressed using equation (1), where $\tilde{v}$ represents frequency in cm^{-1} and d_{et} effective sample thickness in cm as follows:

$$A = 2\pi k \tilde{v} d_{et} \tag{2}$$

Equations (2) and (3) connect both dielectric constants $(\hat{\varepsilon} = \varepsilon' + i\varepsilon'')$ with optical constants ($\hat{n} = n + ik$):

$$\hat{n}^2 = \hat{\varepsilon}, \quad (3a) \qquad \varepsilon'' = 2nk, \quad (3b) \qquad \varepsilon' = n^2 - k^2 \quad (3c)$$

Optical constants can be calculated using K-K transformation, which yields $n(\tilde{v})$ from $k(\tilde{v})$ and vice versa via

$$n(\tilde{v}_a) - n(\infty) = \frac{2}{\pi} \int_0^\infty \frac{\tilde{v} k(\tilde{v})}{\tilde{v}^2 - \tilde{v}_a^2} d\tilde{v},$$

$$k(\tilde{v}_a) = \frac{-2\tilde{v}_a}{\pi} \int_0^\infty \frac{n(\tilde{v})}{\tilde{v}^2 - \tilde{v}_a^2} d\tilde{v} \tag{4}$$

In general K-K transformation connects several frequency depended imaginary and real physical quantities with integral equations. Hence instead of using *n* and *k* the reflectivity R_s and phase angle θ_s can also be used [6].

Since the reflectivity at the interface between a nonabsorbing medium of refractive index n_r and absorbing medium of refractive index n and dielectric constants given by the equations (2) and (3) for parallel polarized light is

$$R_s = \frac{n_r \cos^2\theta - 2an_r \cos\theta + Y}{n_r \cos^2\theta + 2an_r \cos\theta + Y} \qquad (5)$$

where

$$Y = \sqrt{X^2 + \varepsilon''^2}, \qquad a = \frac{1}{2}\sqrt{X+Y} \text{ and } X = \varepsilon' - n_r \sin^2\theta. \qquad (6a, b, c)$$

For detailed analyses and comparison between the calculated reflectivity (R_s) and experimental spectrum (ATR), we have to know their mutual dependence[3]

$$ATR = -\log_{10}\left[\frac{\left(R_s^m + R_s^{2m}\right)}{2}\right] \qquad (7)$$

with the solution for R_s as

$$R_s = \left[\frac{1}{2}\sqrt{1 + 8ATR} - \frac{1}{2}\right]^{1/m} . \qquad (8)$$

Equation (8) is written for the geometry of CIRCLE ATR cell only (Fig. 1b), where θ is 45° and where reflectivities in both polarizations are related as $R_p = R_s^2$. This relation is used during the iterative procedure of calculating the n and k by K-K transformation when the calculated values are compared with the uncorrected spectrum. In general, the system of Fresnel equations must be solved for the given optical system to get the relation between the spectrum and reflectivity.

Results and discussion

Two typical ATR experiments are shown in Figure 1. The first one represents a horizontal ATR plate covered with a sample. All kinds of samples can be measured using a horizontal ATR cell, from solids through pastes to liquids. The only limitation is, as in all ATR experiments, that we have to ensure as good as possible optical contact between the sample and the IRE. Usually it is easy to fulfill this condition, especially

when liquid samples or films built up directly on the IRE are used. Difficulties start up with solid samples. We have two possibilities to overcome the problems with the contact area when solid samples are used. First one is to apply so-called a mouse trap, i.e. a solid cover where the pressure of the sample on IRE can be precisely regulated. With constant pressure the reproducibility of ATR spectra is fulfilled. Second possibility is to use of nujol (similar as in the transmittance experiment), which serve as a matrix to allow better optical contact between the solid sample and IRE[7].
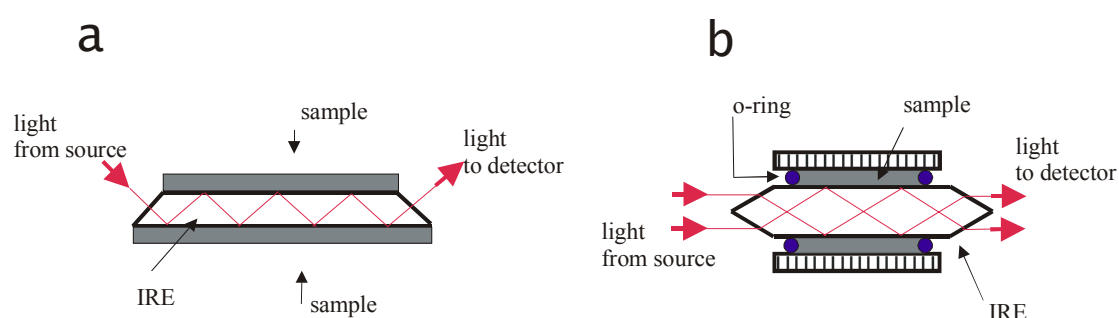

Figure 1. A horizontal geometry of ATR cell and b. CIRCLE ATR cell for liquid samples.

For liquids, a specially designed CIRCLE ATR cell can be used. Besides its simple geometry, its main advantage is that it guarantees very effective optical contact between the sample and IRE. It possesses a very high degree of symmetry, and hence makes calculation of optical constants easier. A convenience of the CIRCLE ATR is that, provided the light beam is symmetrical with respect to the rod, the ratio of s- and p-polarized light is 1:1, regardless of the polarization discrimination of the instrument[3].

Table 1. Band frequencies of OH stretching (ν OH) and OH bending mode (δ OH) of liquid water for various types of spectra (in cm^{-1}).

	ν *OH*	δ *OH*
transmission	3407	1644
uncorrected ATR	3337	1636
corrected ATR	3336	1635
calculated absorbance	3406	1644
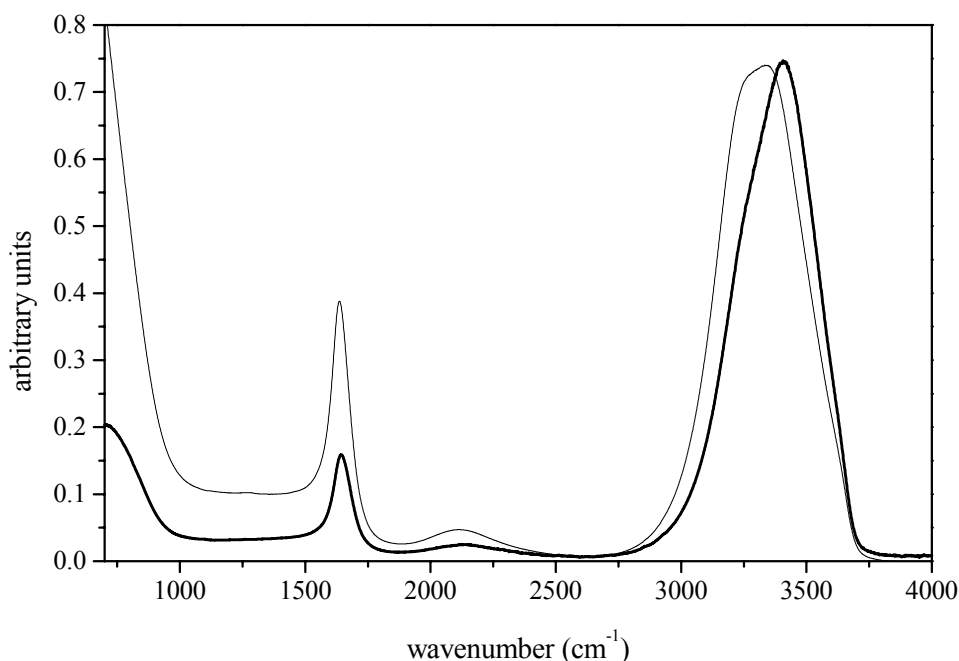
**Figure 2**. The IR spectrum of liquid water recorded with a 2 μm thick liquid cell with ZnSe windows in transmission mode (thick line) and uncorrected ATR spectrum (thin line) both normalized to the same height of the OH stretching mode.

In this article all measurements and consequently calculations were made for this type of ATR cell. Several types of material with high refractive indices for IRE are used in both types of cells. Most frequently used are ZnSe (n_r=2.4 at 1000 cm^{-1}), AMTIR (GeAsSe glass, n_r=2.5 at 1000 cm^{-1}), Si (n_r=3.4 at 1000 cm^{-1}) and Ge (n_r=4.0 at 1000 cm^{-1}). A difference in refractive indices between the IRE and sample defines various penetration depths following the equation 1.
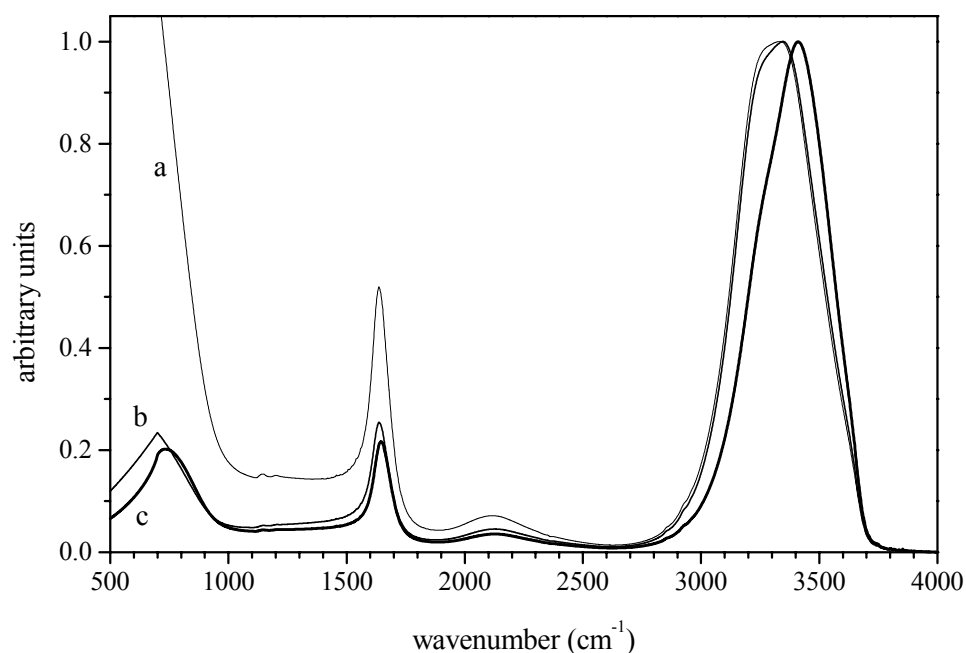
A spectrum of liquid water is a very illustrative example of the distortions on band shape and frequency due to anomalous dispersion. Details are presented in Figures 3 and 4 and in Table 1. The main distortion can be observed in the region of OH stretching mode. Table 1. The main distortion can be observed in the region of OH stretching mode.

The band maximum shifted to lower frequency for 70 cm^{-1} with the corresponding red shift of its centre of gravity. The changes in the OH bending mode are less pronounced, except the change in the relative intensity. With the ATR correction, which is usually available in commercial software, only the adjustment for the wavelength dependence of penetration depth is taken into account. The effects of this calculation are presented in Figure 5. This kind of calculation (using equation 1) adjusts the relative intensity in the whole spectrum region to become comparable to the transmission spectrum. But it does not alter the band shapes, which remain almost the same.
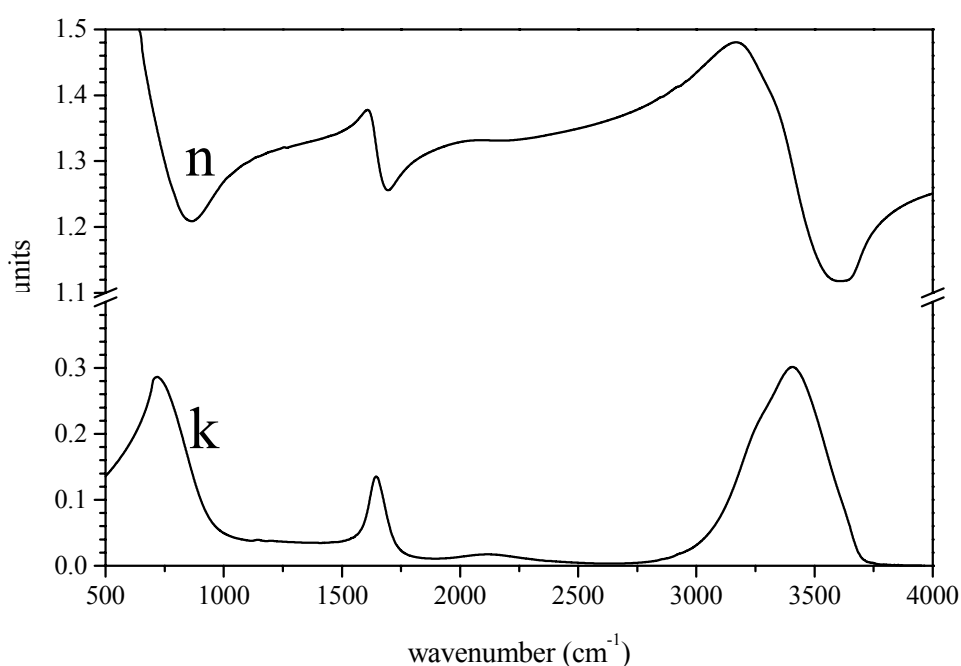
Figure 3. Calculated *n* and *k* of pure water from the spectrum shown in Fig.2. Values of both optical constants are the same as previously calculated in Refs.[6,3,8]

To obtain a spectrum, which is also comparable in bandshape with the spectrum in transmission set up, the optical constants *n* and *k* should be calculated first. In Figure 3 are drawn both constants, calculated with the K-K transformation for optical system in CIRCLE ATR cell. Once *n* and *k* are known, it is trivial to calculate absorbance spectrum using equation 1 or dielectric constants calculated from equations 3a and 3b.
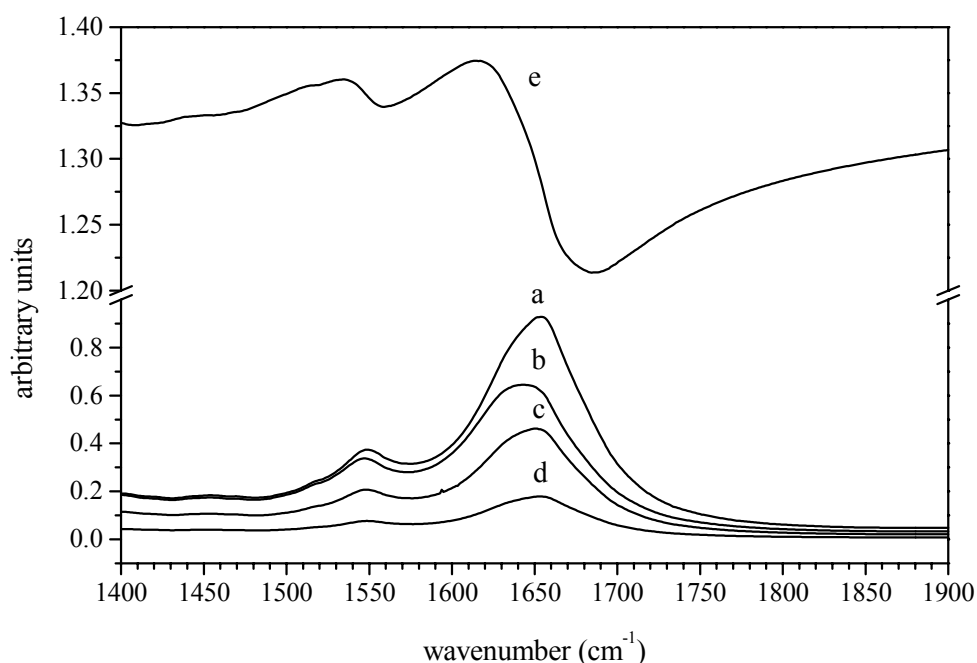

Figure 4. **a**. An uncorrected ATR spectrum of liquid water, **b**. a corrected ATR spectrum using commercial software and **c**. a calculated spectrum from optical constants

Another illustrative example of the band distortion when using experimental ATR set up represents the spectra of BSA protein in buffer solutions[9,10]. It is well known that from the IR spectra of proteins, the secondary structure of proteins can be determined[11-13]. Especially useful for this purpose is the Amide I band[11,12], which is, in the case of folded proteins, composed of several bands. These bands belong to vibrations of different classes of secondary structure elements. These bands are usually evaluated with a band fitting algorithm and/or Fourier self deconvolution[14,15]; the frequency of the components determine the type of secondary structure (α *helix*, β *sheet* and various types of turns), while the area of these bands is connected to the population of secondary

elements in the whole protein molecule[11,12]. Hence, for precise structural determination, the exact knowledge of the shape as well as the frequency of the Amide I band is prerequested. From Fig. 6 it is obvious that anomalous dispersion of real refractive index n has dramatic effects on the shape, as well as on the frequency, of both Amide I and Amide II bands. It can be noticed that without the use of resolution enhancement techniques such as second derivative spectroscopy and Fourier deconvolution technique that decomposition of both Amide I and II bands would yield completely different results.


Figure 5. The Amide I and II region of protein spectrum (BSA, 2.4 mM solution in phosphate buffer, ATR CIRCLE cell) after subtraction of phosphate buffer. a. a calculated absorption spectrum d=0.5μm, b. an uncorrected ATR spectrum (CIRCLE cell), c. calculated imaginary part (ε'') of $\hat{\varepsilon}$, d. calculated k, and e. calculated n.

It has to be emphasized, that among the mentioned mechanisms of band distortion, the solvent subtraction (in our case phosphate buffer) can also disrupt the structure of the Amide I band. Namely the OH bending band at 1640 cm^{-1} is strongly overlapped with

Amide I band. Only the bulk phosphate buffer can be successfully subtracted, which is not influenced by the presence of the protein molecules.

The differences in the shape and frequencies can also be observed in the Amide II region and in the high frequency region of the Amide I band, i.e. the regions which are not disturbed by the overlapping of the OH bending mode. The difference spectrum, presented in Fig. 6, shows clearly the band distortions in ATR spectrum.
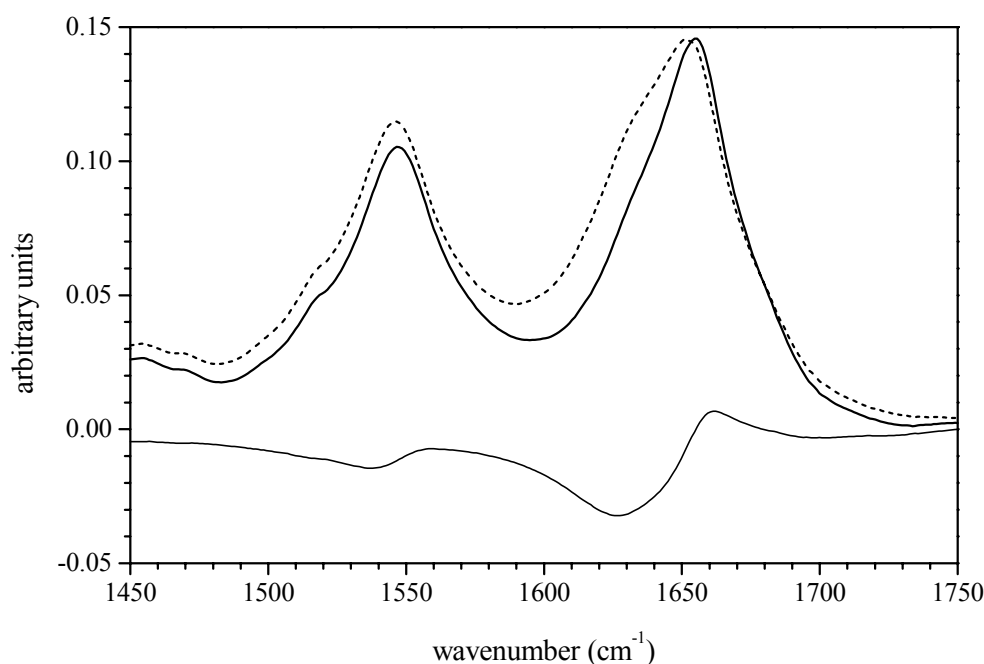
 Figure 6. The Amide I and II regions of BSA in the uncorrected ATR spectrum (dashed line) and calculated absorption spectrum (solid line). Phosphate buffer is subtracted and uncorrected ATR spectrum is corrected for wavelength dependence of the depth of light penetration using commercial ATR correction (Eq. 1). The bottom spectrum represents the difference between the upper ones.

The band area of Amide I in ATR spectrum, previously corrected for wavelength dependence of light penetration into the sample, is approximately 10% larger than in the calculated one. Since the secondary structure determination of proteins using IR transmission spectra can be calculated with a relative error smaller that 5%, these refraction distortions are the source of the main inaccuracy in structure determination.

This problem, as it was demonstrated, can be simply overcome with the calculation of optical constants.

Conclusions

IR transmission technique is still widely used in routine as well as in research FTIR spectroscopy. Besides its very simple use and universality, the frequencies of bands and the band shape are directly related to microscopical physical quantities and hence prepared for interpretation at once. However, the development of the FTIR accessories and fast grown research areas of biological significance apply to systems of interest where water is the most important solvent. Water solutions and water itself have been for many years assumed as "poison" for infrared spectroscopy, and only since the application of ATR techniques relevant spectra can be recorded. With this technique a whole mid-infrared spectrum can be used without any restrictions due to saturation effects of the OH vibrational bands. The only drawback is that the ATR spectra need further processing in order to get physical significance on a molecular level. This can be easily achieved with the calculation of optical constants using well-known K-K transformation. From the two examples described in this paper it can be deduced that the calculation of optical constants is mandatory when an ATR set up of FTIR experiments is used. Although there are some obscurities with the calculation of optical constants using the K-K transformation (spectrum is measured in a finite interval, usually only approximate value of n_∞ is known, imperfections of optical instrumentation), the similarity between the spectra calculated from the optical constants and the spectra measured in transmission technique is better than 10^{-3} absorbance unit or even better, if we are able to mathematically describe and/or avoid or at least alleviate some of the mentioned difficulties in the procedure of calculating the optical constants. This is also one of the reasons why is a CIRCLE ATR cell so widely used. Its cylindrical symmetry, $45°$ incidence angle and simple but highly refined optics are characteristics, which allow us to calculate a spectrum even more accurately. To obtain such good a quality ATR spectrum that ensures further accurate calculation of the optical constants, some readjustments of the cell are prerequisite. A methodology of calculating *n* and *k* for CIRCLE and horizontal ATR (both optical path are presented in Fig. 1) will be evaluated and precisely described in a forthcoming paper.

References and Notes

1. Fahrenford, J. *Spectrochimica Acta* **1961,** *17*, 698.
2. Harrick, N. J. *Internal Reflection Spectroscopy*; Interscience Publisher: New York London Sydney, 1967.
3. Bertie, J. E.; Eysel, H. H. *Applied Spectroscopy* **1985,** *39*, 392–401.
4. Bertie, J. E.; Ahmed, M. K.; Eysel, H. H. *J. Phys. Chem.* **1989,** *93*, 2210–2218.
5. Bertie, J. E.; Zhang, S. L. *Can. J. Chem.* **1992,** *70*, 520–531.
6. Bertie, J. E.; Lan, Z. *J. Chem. Phys.* **1996,** *105*, 8502–8514.
7. Kuenzelmann, U.; Neugebauer, H.; Neckel, A. *Langmuir* **1994,** *10*, 2444–2449.
8. Maréchal, Y. *J. Chem. Phys.* **1991,** *95*.
9. Grdadolnik, J.; Maréchal, Y. *Biopolymers (Biospectroscopy)* **2001,** *62*, 54–67.
10. Grdadolnik, J.; Maréchal, Y. *Biopolymers* **2001,** *62*, 40–53.
11. Krimm, S. *J. Mol. Biol.* **1962,** *4*, 528–540.
12. Krimm, S.; Bandekar, J. *Adv. Prot. Chem.* **1986,** *38*, 181–264.
13. Miyazawa, T. *J. Chemical Physics* **1960,** *32*, 1647–1652.
14. Mantsch, H. H.; Casal, H. L.; Jones, R. N. In *Advances in Spectroscopy;* Clark, R. J.; Hester, R. E. Eds.; John Wiley and Sons: Chichester New York Brisbane Toronto Singapore, 1986; Vol. 13; pp. 1–42.
15. Kauppinen, J. K.; Moffatt, D. J.; Mantsch, H. H.; Cameron, D. G. *Appl. Spectrosc.* **1981,** *35*, 1454.

Povzetek

V članku so opisane prednosti in slabosti ATR-FTIR spektroskopije. Kot primer smo obravnavali infrardeče spektre tekoče vode in raztopino proteina BSA v fosfatnem pufru. Na obeh primerih so prikazane temeljne razlike v spektrih posneti v običajni transmisijski in ATR tehniki. Podane so enačbe, s katerimi lahko iz ATR spektra izračunamo optični konstanti n in k, ter čisti absorbcijski spekter. Tako izračunani spekter je popolnoma enak spektru posnetemu v transmisijski tehniki, brez anomalij, ki so posledice anomalne disperzije, zaradi frekvenčne odvisnosti realnega dela lomnega količnika (n). Izračuni optičnih konstant so izpeljani za primer cilindrične simetrije v CIRCLE ATR celici.